*THE EXTRACELLULAR NUCLEASE OF STAPHYLOCOCCUS AUREUS: STRUCTURES OF THE NATIVE ENZYME AND AN ENZYME-INHIBITOR COMPLEX AT 4 Å RESOLUTION**

By Arthur Arnone,† C. James Bier, F. Albert Cotton, Edward E. Hazen, Jr., David C. Richardson, and Jane S. Richardson

DEPARTMENT OF CHEMISTRY, MASSACHUSETTS INSTITUTE OF TECHNOLOGY, CAMBRIDGE, MASS. 02139

Communicated May 6, 1969

Abstract.—Independent 4 Å electron density maps calculated for the extracellular nuclease of *Staphylococcus aureus* (based on data from three heavy-atom derivatives) and for a nuclease-thymidine-3′,5′-diphosphate-calcium ion complex (based on a single isomorphous derivative) show about 60 per cent of the chain resolved, including $3^1/_2$ turns of helix. The pyrimidine ring of the inhibitor fits into a pocket in the enzyme and appears to be parallel to the ring of a tyrosyl residue. Conformational changes can be observed between the nuclease and the nuclease-inhibitor complex, but the two structures seem to be identical over most of the molecule.

The extracellular nuclease of *Staphylococcus aureus*, a calcium ion-activated enzyme that attacks the phosphodiester bonds of both RNA and DNA, consists of a single chain of 149 amino acid residues (mol. wt. = 16,807) with no sulfhydryl or disulphide groups. C. B. Anfinsen and his associates have recently reviewed[1] their extensive work on the chemistry of this nuclease, including a sequence determination and progress toward total synthesis. We previously reported the crystallization of the nuclease in several forms[2]; the present paper describes our further progress with an X-ray crystallographic determination of the structure.

Methods and Results.—Nuclease (Foggi strain) was purchased from Worthington Biochemical Corp. Used material was recovered and preparations that gave poor crystals were reworked, originally by recrystallization, but more recently by chromatography on phosphocellulose.[3] As previously described,[2] uninhibited nuclease crystals were grown in siliconed vials at 2°C from a 1–2 mg/ml solution of nuclease in pH 8.15, 0.0105 M potassium phosphate buffer with 2-methyl-2,4-pentanediol[4] added dropwise to a final concentration of 29–32 per cent and a final pH (at 25°) of 8.6–8.7. Good crystals formed in 1–2 months; they were tetragonal, space group $P4_1$, of unit cell dimensions a = 47.75, c = 63.5 Å. For nuclease-inhibitor crystals, a solution of enzyme and buffer (as above) with 22–25 per cent diol was allowed to stand at 2°C for several days and then filtered through a 0.45 μ pore-size Millipore filter in a filtering centrifuge tube. One mole per mole nuclease of thymidine-3′,5′-diphosphate (pdTp), a potent inhibitor,[5] was added, and two moles Ca^{2+} in the form of 0.01 M calcium chloride-0.02 M potassium citrate were also added. These crystals grew more rapidly than the native nuclease crystals and were of the same space group but with unit cell dimensions of a = 48.3, c = 63.3 Å. No crystals of either type that varied more than 0.1 Å from the given unit cell dimensions were used. Crystal size ranged from 0.15 × 0.15 × 0.5 mm for some nuclease-pIdUp crystals to 0.4 × 0.5 × 0.7

mm for the largest uninhibited crystals. In some preparations (Fig. 1*b*), the polarity of the fourfold screw axis was evidenced in the external morphology: at one termination the 1,1,1 faces (diamond-shaped) were developed and at the other end the 0,1,1 faces (triangular).

5-Iododeoxyuridine-3′,5′-diphosphate (pIdUp) was prepared by phosphorylating commercial 5-iododeoxyuridine with the 2-cyanoethyl phosphate reagent of the Tener,[6] isolated on a Dowex 2 column,[7] and characterized spectrally and by phosphate analysis.[8] Nuclease crystals containing this material were prepared in the same way as those containing pdTp.

A $PtCl_4^{2-}$ derivative of uninhibited enzyme was prepared by soaking crystals for five days in a solution of 1×10^{-4} M K_2PtCl_4 in the standard phosphate buffer and 40 per cent by weight diol. The crystals were then transferred to a wash solution of buffer and diol. Longer soak times produced multiple-site substitution and unacceptable changes in unit cell dimensions. Eastman p-acetoxymercurianiline (PAMA) was recrystallized from chloroform; uninhibited nuclease crystals

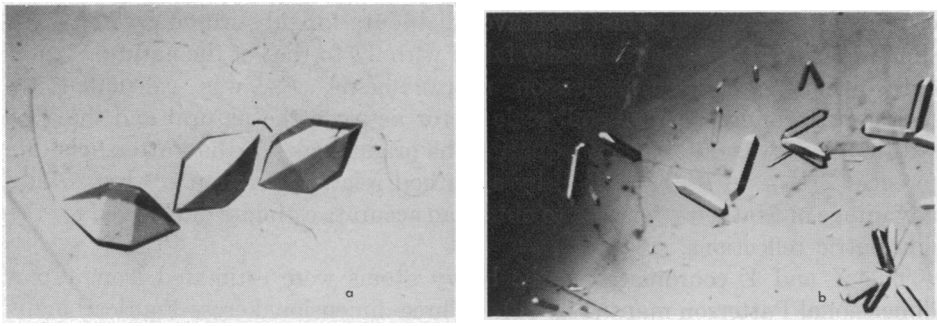

FIG. 1.—Crystals of the nuclease-inhibitor complex. In 1*b*, one end is terminated by the 1,1,1 pyramid (diamond-shaped faces) and the other end by the 0,1,1 pyramid (triangular faces).

were soaked for about a month in a 1×10^{-4} M PAMA solution in the phosphate buffer and 40 per cent diol. Similarly, crystals were soaked in 1×10^{-4} M p-chloromercuribenzene sulfonic acid (PCMBS), but the concentration was then raised in two steps at ten-day intervals to 3×10^{-4} M and maintained for one month at this molarity before crystals were removed for use. The stepwise increase in concentration reduced cracking of the extremely fragile PCMBS-soaked crystals. The heavy atom was in at least ten-fold molar excess over the nuclease in all soaks. In current practice all unsubstituted crystals and substituted crystals grown from solution are equilibrated before use in a 40 per cent diol solution of the appropriate buffer, plus 10^{-4} M Ca^{2+} and 10^{-4} M nucleoside diphosphate for the nuclease-inhibitor crystals.

Crystals were mounted in sealed glass capillaries, and data were collected at 2°C using a carefully aligned,[9] Datex-controlled, General Electric XRD-6 diffractometer with an Electronics and Alloys full-circle goniometer. We have modified this instrument to allow a range of -45 to $+100°$ in 2θ, provided for interchangeable nosepieces on the incident-beam collimator, and added a diffracted-

beam aperture of variable position and size.[10] Intensities were measured by the stationary-crystal, stationary-counter method at a takeoff angle of 6°, using copper radiation and a pair of balanced filters. An additional background correction was applied as a function of 2θ. Absorption correction curves were measured by taking scans of the O,O,l reflections at $\chi = 90°$. For our case of crystals with approximately square cross section, the absorption correction was almost entirely due to the capillary and was the same at $+2\theta$ and -2θ. Ten reflections were measured at $+2\theta$, followed by the Friedel pairs at -2θ, with standard test reflections inserted every 100. A crystal was discarded when the average intensity dropped more than 5 per cent or the unit cell size changed. All independent reflections within the 4 Å sphere were collected (2800, including Friedel pairs). Each reflection of each crystal type was measured at least twice, because we found that anomalous-dispersion differences from a single set of data were not statistically accurate enough to give clean cross-Fourier maps.

After the raw data had been corrected and measurements from separate crystals of the same type had been averaged, data for substituted crystals were shell-scaled to match their intensity falloff with 2θ to that of the natural crystal data. Using anomalous-dispersion measurements, F_H was calculated by Mathews' formula.‡ An overall scale factor between the natural and the substituted data was obtained by equating the origin peaks of the Patterson's difference ($\Sigma(F_{PH}^2 - F_P^2) = \Sigma F_H^2$) by a method related to Kraut's,[12] but taking advantage of Mathews' formula to obtain an accurate estimate of F_H even for the noncentric reflections.

The X and Y coordinates of the heavy atoms were estimated from three-dimensional Patterson maps (Fig. 2*a*). Three-dimensional cross-Fourier[13] maps were used to check the X and Y positions and to determine relative Z coordinates

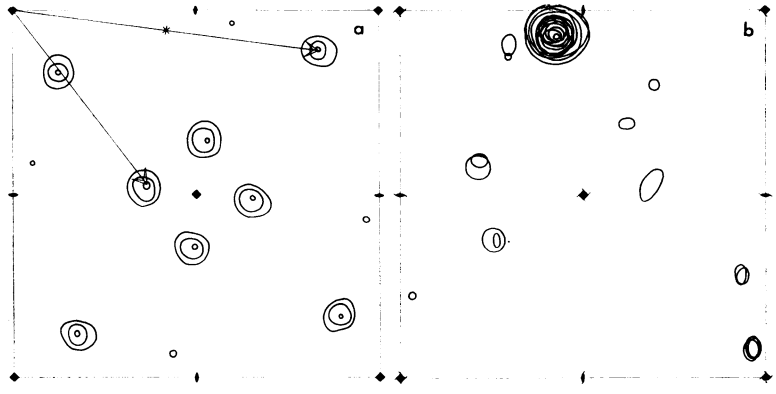

FIG. 2.—Location of the iodine atom of the pIdUp derivative. (a) 3-dimensional Patterson map of F_H^2 (full unit cell in u and v, all sections superimposed from w = 0 to w = 1/2); (b) 3-dimensional cross-Fourier map made using the inhibited-crystal magnitude for F_P and F_{PH} but the native-crystal phase of F_P determined from the $PtCl_4^{2-}$ substitution (full unit cell in x and y, all sections superimposed from z = 0 to z = 1/4).

(Figs. 2*b* and 3*a*). At this step, the anomalous difference was used only to choose between the two possible solutions of the phase triangle for F_H. The first such cross-Fourier was used to choose between space groups $P4_1$ and $P4_3$. Phases for F_P were calculated from the $PtCl_4^{2-}$ substitution and applied to the PAMA data (Figs. 3*a* and 3*b*); when $P4_1$ was assumed the cross-Fourier showed the two close PAMA sites, but when $P4_3$ was assumed, the map showed only random, low-level noise.

Heavy-atom coordinates, relative occupancies, and temperature parameters were refined by standard least-square techniques, using the M.I.T. time-sharing system. Allowance was made during later cycles for centric reflection "cross-overs" through zero[14] and also for the analogous noncentric case of an obtuse angle between F_P and F_{PH}; the "crossover" value is chosen in refinement for (see footnote‡) about 1 per cent of the reflections. Refinement results are summarized in Table 1.

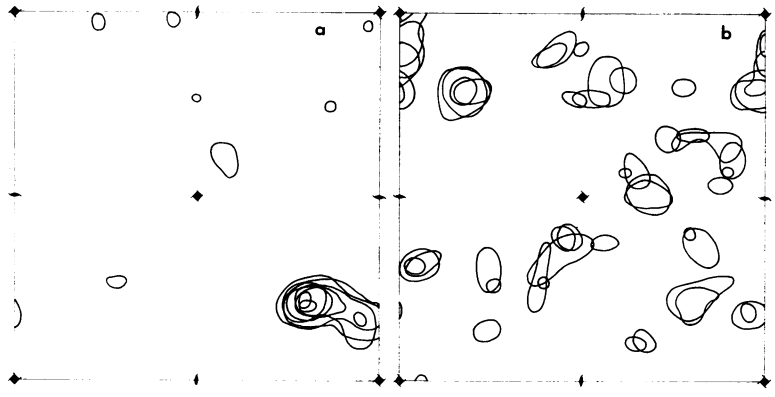

FIG. 3.—Three-dimensional cross-Fourier functions of F_H for PAMA based on F_P phases determined from the $PtCl_4^{2-}$ derivative (full unit cell in x and y, sections superimposed from z = 0 to z = 1/4): (a) assuming spacegroup $P4_1$, (b) assuming spacegroup $P4_3$.

Native-crystal phases were calculated from the centroid of the combined probability distribution as described by Blow and Crick[15] and by Dickerson, Kendrew, and Strandberg.[16] Isomorphous and anomalous distributions were calculated separately as suggested by North[17] to allow for the difference in their root mean square errors. "Best" Fourier maps[15, 16] of the nuclease and of the nuclease-inhibitor complex were generated from these phases. The phases for the nuclease-inhibitor map were based on the single, highly isomorphous substitution of an iodine for the methyl group on the thymidine-3′,5′-diphosphate. Since no information from the uninhibited nuclease data was used in processing the nuclease-inhibitor data except for the choice of a relative Z coordinate for the iodine, the great similarity of the two maps provides strong evidence that both are essentially correct.

An anomalous-difference Fourier map[18] calculated from the unsubstituted nuclease-inhibitor-Ca^{2+} complex data shows a single sharp peak 2–3 times above

TABLE 1. *Summary of refinement results of heavy-atom coordinates, relative occupancies, and temperature parameters as refined by standard least-square techniques.*

	Uninhibited Nuclease	$PtCl_4^{2-}$	PAMA*	PCMBS*	Nuclease-pdTp Ca^{2+} complex	Nuclease-pIdUp Ca^{2+} complex
Average crystal size in mm	0.7 × 0.5 × 0.4	0.7 × 0.4 × 0.3	0.6 × 0.4 × 0.3	0.4 × 0.3 × 0.2	0.8 × 0.3 × 0.2	0.8 × 0.15 × 0.15
Relative average intensity	9.5	2.6	2.2	1.6	3.6	1.0
Residual among crystals	2%	6%	4%	6%	2%	6%
$R = \Sigma(F_{PH} - F_P)/\Sigma F_P$		24%	15%	29%		23%
$Sca = \Sigma F_{PH}^2/\Sigma F_P^2$		1.09	1.11	1.20		1.10
k = real F_H/imag F_H		9.0	11.4	11.6		8.9
Heavy atom		Pt	Hg1 Hg2	Hg1 Hg2 Hg3	Ca	I
Relative occupancy		1	1 0.43	1 1.02 1.02	1	1
X		0.67	0.77 0.85	0.80 0.86 0.85	0.12	0.06
Y		0.51	0.81 0.96	0.80 0.94 0.63	0.28	0.41
Z		0.04	0.14 0.12	0.13 0.10 0.14	0.26	0.34
B_{iso}		2.5	6.1 9.2	7.6 27.3 24.3		2.7
$R = \Sigma (F_H ob - F_H calc)/\Sigma F_H ob$		51%	52%	50%		39%
root mean square iso. error		9.5	5.5	9.0		5.8
root mean square anom. error		2.1	1.4	1.9		3.0
Σ FIGM$(\Phi_{sub} - \Phi_{best})/\Sigma$ FIGM†		34°	42°	43°		

*PAMA, *p*-acetoxymercurianiline; PCMBS, *p*-chloromercuribenzine sulfonic acid; pdTp, thymidine-3′,5′-diphosphate; pIdUp, 5-iododeoxyuridine-3′,5′-diphosphate.

† FIGM is the figure of merit and Φ_{sub} is the centroid phase from the combined isomorphous and anamalous probability distributions of the single derivative. Φ_{best} is the phase from all three derivatives combined.

background (Fig. 4). We assigned this to a Ca^{2+}, since the bound Ca^{2+} was the strongest anomalous scatterer in these crystals and this was the same position where a single barium atom had been located in another set of substitution trials. Working at higher pH than that used in growing the crystals, Cuatrecasas *et al.*[19] have shown that a second calcium ion is also involved in pdTp binding, but we have found no indication of it.

Discussion.—From a 6 Å electron density map of the native nuclease, the boundaries of a molecule could be determined (as in the styrofoam model, Fig. 5) and there were indications of where helical sections of chain and the binding site might be located.

By comparing the 4 Å maps of the native and the inhibited nuclease, the binding site of the pdTp could be located quite unambiguously in the area to the top left front in Figure 5. The added electron density can be fitted in considerable detail: the pyrimidine ring of the pdTp fits into the well-defined "pocket," with the 3′-phosphate toward the top of the molecule and the 5′-phosphate down close to the Ca^{2+} position (see Fig. 6). The pyrimidine ring is parallel to and about 3.5 Å from what we tentatively identify as the ring of a tyrosine residue, both from its shape and because Cuatracasas *et al.*[20] have shown that binding of thymidine-3′,5′-diphosphate dramatically affects the reactivity of two of the tyrosine residues. Upon inhibitor binding, the side chains of this residue and an adjacent one appear to rotate about 90°, aligning the tryosine ring parallel to the pyrimidine ring of the thymidine-3′,5′-diphosphate. Figure 7 shows the comparison between the two maps in that region. Several other small, less well defined, conformational changes appear to occur near the inhibitor binding site.

Along the right bottom side of the molecule from front to back is a clearly

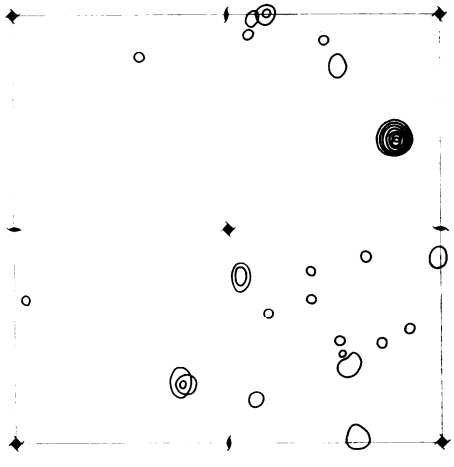

FIG. 4.—Anomalous-difference Fourier map of $F_P{}^+$-$F_P{}^-$ from the unsubstituted nuclease-inhibitor crystals (full unit cell in x and y, all sections superimposed from z = 0 to z = 1/4). The highest peak is the presumed Ca^{2+} position.

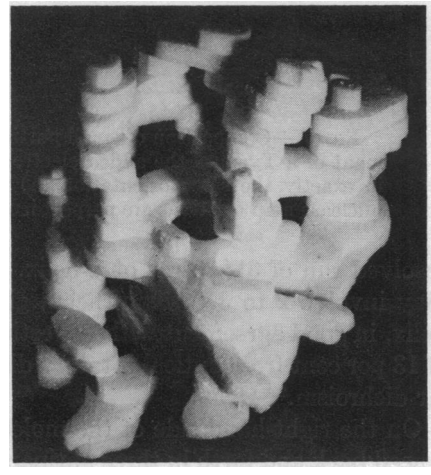

FIG. 5.—Styrofoam model constructed from the electron-density map of the native nuclease at 6 Å resolution.

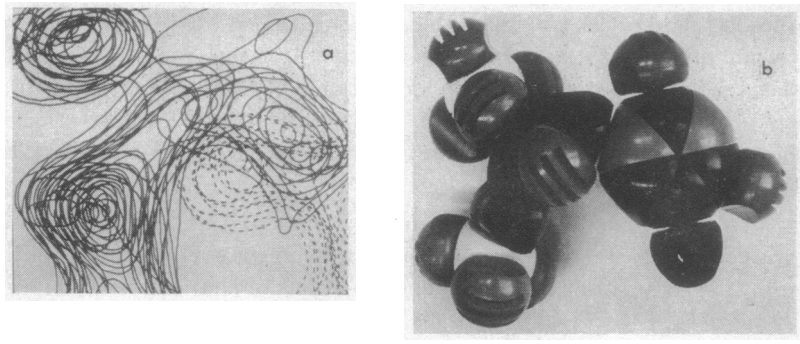

FIG. 6.—A comparison of (a) the observed contours (solid lines) defining what we identify as the bound inhibitor molecule, thymidine-3',5'-diphosphate, and (b) a space filling model of pdTp. The dotted contours in (a) correspond to what we assign as a tyrosine residue.

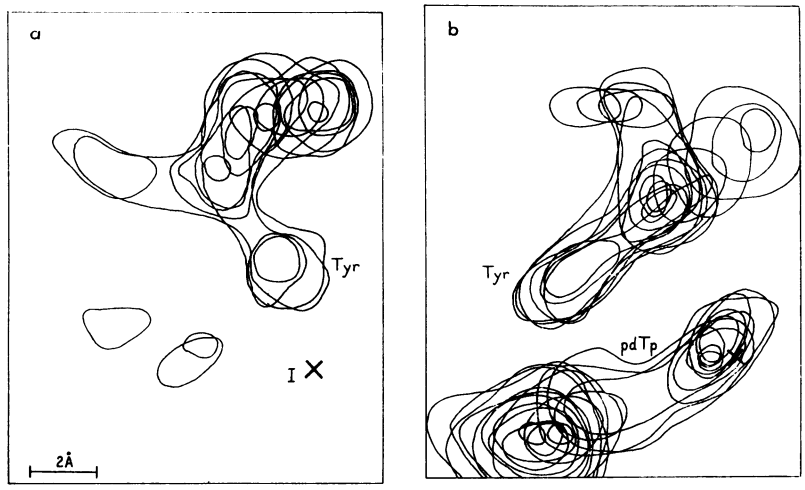

FIG. 7.—Comparison of small portions of the two 4Å maps, showing the movement of a Tyr and the added electron-density of the pdTp. The two maps are in exactly the same orientation (a) the native nuclease map (b) the inhibited nuclease map (sections are perpendicular to those in 6a).

resolved run of $3^1/_2$ turns of α-helix. There is another less clear section which may involve 2 to 3 turns of helix, giving a total of approximately 15 per cent helix, in good agreement with the estimates obtained from optical measurements of 13 per cent from optical rotatory dispersion techniques to 18 per cent by circular dichroism.[21]

On the right-hand side of the molecule, as seen in Figure 5, the chain can be traced back and forth in three antiparallel sections which form an almost vertical sheet above the helix. The path of the backbone chain can be readily followed for about two-thirds of its length, but in several places the connectivity is unclear.

We are greatly indebted to C. B. Anfinsen and his associates for their continual help and encouragement.

* Supported by an NIH grant GM 13300 and a grant from the Research Corporation to E. E. H.

† NIH Predoctoral Fellow.

‡ $(F_H^2 = F_P^2 + F_{PH}^2 \pm 2F_PF_{PH}\{1 - [wk(F_{PH}^+ - F_{PH}^-)/2F_P]^2\}^{1/2}$, w = 0.75: the minus sign is the normal version[11]; we use the plus sign for the "crossover" cases.

[1] Cuatrecasas, P., H. Taniuchi, C. B. Anfinsen, and D. Ontjes, *Brookhaven Symposia in Biology*, No. 21 (1968), p. 172.

[2] Cotton, F. A., E. E. Hazen, Jr., and D. C. Richardson, *J. Biol. Chem.*, **241**, 4389 (1966).

[3] Fuchs, S., P. Cuatrecasas, and C. B. Anfinsen, *J. Biol. Chem.*, **242**, 4768 (1967).

[4] King, M. V., *Biochem. Biophys. Acta*, **79**, 388 (1964).

[5] Cuatrecasas, P., S. Fuchs, and C. B. Anfinsen, *J. Biol. Chem.*, **242**, 1541 (1967).

[6] Tener, G. M., *J. Am. Chem. Soc.*, **83**, 159 (1961).

[7] Lipkin, D., R. Markham, and W. H. Cook, *J. Am. Chem. Soc.*, **81**, 6075 (1959).

[8] Ames, B. N., in *Methods in Enzymology*, eds. E. F. Neufeld and V. Ginsburg (New York: Academic Press, 1966), vol. 8, p. 115.

[9] Richardson, D. C., and A. Parkes, unpublished techniques.

[10] Designed and fabricated by E. T. Tarpin, 10 Tarpin Terrace, Reading, Mass.

[11] Mathews, B. W., *Acta Cryst.*, **20**, 230 (1966).

[12] Kraut, J., L. C. Sieker, D. F. High, and S. T. Freer, these PROCEEDINGS, **48**, 1417 (1962).

[13] Dickerson, R. E., M. L. Kopka, J. C. Varnum, and J. E. Weinzierl, *Acta Cryst.*, **23**, 511 (1967).

[14] Lunberg, B., *Acta Cryst.*, **18**, 576 (1965).

[15] Blow, D. M. and F. H. C. Crick, *Acta Cryst.*, **12**, 794 (1959).

[16] Dickerson, R. E., J. C. Kendrew, and B. E. Strandberg, *Acta Cryst.*, **14**, 1188 (1961).

[17] North, A. C. T., *Acta Cryst.*, **18**, 212 (1965).

[18] Strahs, G., and J. Kraut, *J. Mol. Biol.*, **35**, 503 (1968), and J. Kraut in the appendix to this paper.

[19] Cuatrecasas, P., S. Fuchs, and C. B. Anfinsen, *J. Biol. Chem.*, **242**, 3063 (1967).

[20] Cuatrecasas, P., S. Fuchs, and C. B. Anfinsen, *J. Biol. Chem.*, **243**, 4787 (1968).

[21] Taniuchi, H., and C. B. Anfinsen, *J. Biol. Chem.*, **243**, 4778 (1968).